Phase-shift analysis of two-dimensional carrier-carrier scattering in GaAs and GaN: Comparison with Born and classical approximations

Antónia Mošková and Martin Moško
Institute of Electrical Engineering, Slovak Academy of Sciences, Dúbravská cesta 9, SK-842 39 Bratislava, Slovak Republic
(Received 30 December 1998; revised manuscript received 4 June 1999)

We study Markovian two-dimensional (2D) carrier-carrier (c-c) scattering in GaAs and GaN quantum well systems. We evaluate the phase shifts of scattered partial waves by numerically solving the Schrödinger equation for the 2D c-c collision problem. The output of this ''phase shift analysis'' is exact quantum results (in Markovian limit) for the 2D c-c scattering cross section and 2D c-c scattering rate. We compare these results with the results of the Born approximation (with the ''Fermi-golden-rule based'' theory), and find that the Born approximation can strongly overestimate the exact results. In particular, the 2D c-c scattering rate is overestimated by a factor of 1 to 15 in the GaAs quantum well and by a factor of 2 to 100 in the GaN quantum well, if conditions typical for a quantum-well-laser device or for a quantum well excited by a short laser pulse are considered. Our study is performed for a statically screened intercarrier interaction, but we expect the dynamic screening to further deteriorate the Born approximation: We show that the weaker the screening the worse the Born approximation in a 2D system. We also analyze the 2D c-c collision as a classical event, and find a very good agreement with the phase-shift analysis in the case of weak screening. For unscreened 2D c-c collisions the hierarchy of exact, Born, and classical cross sections is derived analytically, and it is shown that the Born approximation breakdown is due to the carrier two dimensionality.

I. INTRODUCTION

Carrier-carrier scattering in semiconductors is responsible for the thermalization of the nonthermal carrier distribution toward a Fermi distribution at elevated carrier temperature,[1,2] for dephasing of ballistic electrons in a degenerate electron gas,[3,4] for the intercarrier Coulomb drag,[5] and for other effects of fundamental interest (for a review, see, e.g., Ref. 6). It also affects the performance of various semiconductor devices, in particular of small silicon metal-oxide-semiconductor field-effect transistors[7] and of semiconductor-quantum-well lasers.[8] Therefore, there is a strong motivation to develop a quantitatively reliable theory of carrier-carrier (c-c) scattering.

In a Fermi gas with many-body Coulomb interaction the concept of c-c scattering emerges from the Landau-Fermi-liquid theory.[9] In that theory singleparticle states (quasiparticles) are defined in a one-to-one correspondence with the single-particle states of the noninteracting gas, except that they are renormalized by the many-body interaction. However, the many-particle wave function created from such quasiparticle states is not an exact solution (a stationary eigenstate) of the many-body Schrödinger equation. This implies that the lifetime of the quasiparticle excitation is finite, i.e., that there is an interaction between the quasiparticles themselves, which scatters them from one single-particle state to another one. The interaction between the quasiparticles is a renormalized (screened) Coulomb interaction and the scattering is (usually[9–14]) represented by successive two-body collision events.

In a so-called Markovian limit, in which the colliding quasiparticle does not ''remember'' the preceding collision, the time evolution of the carrier distribution function due to the two-body collisions is described by the Boltzmann transport equation[15–17] or by the Monte Carlo simulation[18–23] (which is a physically equivalent[24] Markovian approach). A central quantity of the Markovian theory is the two-body collision probability, which is usually calculated in the Born approximation—the perturbation theory in second order in the intercarrier interaction. In the Born approximation, and for the intercarrier interaction screened in the random phase approximation (RPA), the two-body collision probability comes out as a standard ''Fermi-golden-rule'' expression, which simplifies further calculations[12–23] (the nonrandom-phase-approximation contribution to the golden rule has also been considered,[25] still in the second order in the intercarrier interaction).

However, we have pointed out recently[18,26] that in case of two-dimensional (2D) c-c scattering the Born approximation inherently overestimates the 2D c-c scattering rate in the limit of low carrier densities and low collisional energies, i.e., at least in that case the Born approximation should be abandoned and the 2D c-c collision should be analyzed nonperturbatively. (One of us, with co-worker, also pointed out that a similar problem exists in 1D systems.[27])

In this work we study Markovian 2D c-c scattering in a semiconductor quantum well nonperturbatively by means of phase-shift analysis. The analysis is performed for the intercarrier interaction determined from a simple RPA screening model. We express the 2D c-c scattering cross section through phase shifts of scattered partial waves, and extract the phase shifts from an exact solution of the Schrödinger equation for the 2D c-c collision problem. We obtain exact quantum results for the 2D c-c collision cross section and 2D c-c collision rate, which we compare with the Born approximation. *For various conditions of practical importance we find that the Born approximation can fail to describe the 2D c-c scattering in the GaAs and GaN quantum-well sys-*

tems, and we show that the failure is due to the carrier two dimensionality. We also consider the 2D c-c collision as a classical event, and find good agreement with the exact approach in the weak screening limit.

In Sec. II we define the 2D *c-c* collision problem, and discuss its exact analytical solution for a bare Coulomb potential. In Secs. III and IV, the phase-shift analysis is introduced and the 2D *c-c* collision problem is solved exactly (numerically) for a screened Coulomb potential. In Sec. V the 2D *c-c* scattering rate in GaAs and GaN is evaluated under conditions typically encountered in a quantum-well laser and also under conditions characteristic of a quantum well excited by a short laser pulse. The classical analysis of the 2D *c-c* collision is presented in the Appendix.

II. TWO-BODY COLLISION PROBLEM IN TWO DIMENSIONS: INTRODUCTION

As is customary for the Landau–Fermi liquid[9–14] and the Boltzmann equation approach,[15–23] we assume that only the two-body collision events are operative in the 2D plasma. We ignore three-body or even many-body collision events, which are only important in 1D systems.[28,29]

We focus on intrasubband 2D *c-c* collisions in the plasma of electrons and/or heavy holes occupying the lowest quantum-well subband. The reasons why we focus on the situation when only the ground subband is occupied are the following. First, this situation is characteristic of many different experiments which probe 2D *c-c* scattering.[2–6] Second, the situation is relatively simple to analyze in comparison with a multisubband case. Third, even in this simple situation the 2D *c-c* scattering has so far been analyzed in the Born approximation, and there has been no attempt to perform a nonperturbative analysis.

In the intrasubband 2D *c-c* collision a carrier γ changes its in-plane wave vector from $\mathbf{k}$ to $\mathbf{k}'$ by collision with a carrier δ which is scattered from $\mathbf{k}_0$ to $\mathbf{k}_0'$. Call the effective mass of the first carrier m_γ (m_δ), where $\gamma=e,h$ $(\delta=e,h)$. As is customary,[18,30] we define the reduced mass $\mu=2m_\gamma m_\delta/(m_\gamma+m_\delta)$ and the relative wave vectors before and after the collision, $\mathbf{g}=\mu(\mathbf{k}_0/m_\delta-\mathbf{k}/m_\gamma)$ and $\mathbf{g}'=\mu(\mathbf{k}_0'/m_\delta-\mathbf{k}'/m_\gamma)$, respectively. Due to the energy and momentum conservation, one has $|\mathbf{g}'|=|\mathbf{g}|$, so that if the scattering angle ϕ between $\mathbf{g}$ and $\mathbf{g}'$ is known, the final states $\mathbf{k}'$ and $\mathbf{k}_0'$ are determined. Further, it is useful[30] to separate the center-of-mass motion of the colliding carriers from their relative motion, and to consider only the Schrödinger equation for the relative motion. In our 2D case this reads

$$\left[-\frac{\hbar^2}{\mu}\left(\frac{\partial^2}{\partial r^2}+\frac{1}{r}\frac{\partial}{\partial r}+\frac{1}{r^2}\frac{\partial^2}{\partial\phi^2}\right)+V(r)\right]\Phi(r,\phi)=\frac{\hbar^2g^2}{4\mu}\Phi(r,\phi), \tag{1}$$

where r is the in-plane distance between the carriers, the scattering angle ϕ plays the role of a polar angle, $V(r)$ is the effective 2D *c-c* interaction, $\Phi(r,\phi)$ is the wave function of the relative motion, and $\hbar^2g^2/4\mu$ is the eigenenergy. Equation (1) is formally identical, e.g., with the 2D exciton Schrödinger equation,[31] except that now we are interested in unbound states, for which the eigenenergy equals the kinetic energy of the relative motion before (or after) the collision, $\hbar^2g^2/4\mu$.

For a systematic derivation of Eq. (1), one has to consider the 3D Hamiltonian

$$H=-\frac{\hbar^2}{2m_\gamma}\frac{\partial}{\partial z^2}+\Omega_\gamma(z)-\frac{\hbar^2}{2m_\delta}\frac{\partial^2}{\partial z_0^2}+\Omega_\delta(z_0)-\frac{\hbar^2}{\mu}\left(\frac{\partial^2}{\partial r^2}+\frac{1}{r}\frac{\partial}{\partial r}+\frac{1}{r^2}\frac{\partial^2}{\partial\phi^2}\right)+W(r,z-z_0), \tag{2}$$

where z (z_0) is the position of the first (second) carrier in the quantum-well-growth direction, $\Omega(z)$ is the confinement potential, and $W(r,z-z_0)$ is the 3D *c-c* interaction. The restriction to the lowest subband means the use of the wave-function ansatz $\Psi(r,\phi,z,z_0)=\Phi(r,\phi)\chi_\gamma(z)\chi_\delta(z_0)$, where χ_γ and χ_δ are the envelope functions of the carriers γ and δ, respectively. Application of the variational principle to the functional $\langle\Psi|H|\Psi\rangle$ gives the Schrodinger equation (1), with

$$V(r)=\int_{-\infty}^{\infty}dz\int_{-\infty}^{\infty}dz_0\chi_\gamma^2(z)W(r,z-z_0)\chi_\delta^2(z_0). \tag{3}$$

In other words, the 3D problem defined by the Hamiltonian (2) is tranformed into the 2D problem defined by Eq. (1), where the 3D interaction $W(r,z-z_0)$ is replaced by the 2D interaction $V(r)$. Further, since in Eq. (1) the in-plane motion is separated from the motion in the z direction, the potential $\Omega(z)$ is only needed to determine the envelope functions $\chi(z)$ (specified in Sec. III).

For any $V(r)$ which is radially symmetric and becomes zero at $r\to\infty$, Eq. (1) has the asymptotic solution[30]

$$\Phi(r,\phi)_{r\to\infty}=\exp\left(i\frac{\mathbf{g}}{2}\mathbf{r}\right)+\frac{1}{\sqrt{r}}\exp\left(i\frac{g}{2}r\right)f(\phi,g), \tag{4}$$

where $\exp[i(\mathbf{g}/2)\mathbf{r}]$ is the unperturbed plane-wave solution, $1/\sqrt{r}\exp[i(g/2)r]$ is the circular wave due to the scattering, and $f(\phi,g)$ is the the probability amplitude that the carriers are scattered from state $\mathbf{g}$ to state $\mathbf{g}'$ (ϕ is the angle between $\mathbf{g}$ and $\mathbf{g}'$).

The differential scattering cross section (the scattering probability) then reads[30]

$$\sigma(\phi,g)=|f(\phi,g)|^2 \tag{5}$$

for collisions of distinguishable particles $(e\text{-}h)$, while

$$\sigma(\phi,g)=\tfrac{1}{2}\{|f(\phi,g)|^2+|f(\phi+\pi,g)|^2-\tfrac{1}{2}[f(\phi,g)f^*(\phi+\pi,g)+f^*(\phi,g)f(\phi+\pi,g)]\} \tag{6}$$

for collisions of indistinguishable particles $(e\text{-}e,\ h\text{-}h)$. We have derived Eq. (6) following the corresponding 3D derivation.[30] The amplitudes $f(\phi,g)$ and $f(\phi+\pi,g)$ describe the ‘‘direct’’ transition $\mathbf{k}\to\mathbf{k}'$, $\mathbf{k}_0\to\mathbf{k}_0'$ and the ‘‘exchange’’ transition $\mathbf{k}\to\mathbf{k}_0'$, $\mathbf{k}_0\to\mathbf{k}'$, respectively. These transitions are indistinguishable when indistinguishable fermions collide, which gives rise to the interference term (the third term) on the right-hand side of Eq. (6).

We wish to present a calculation of $\sigma(\phi,g)$ which is exact in all orders in the interaction $V(r)$. In general, $V(r)$ is a screened Coulomb potential for which such calculation is complicated (see Secs. III and IV). Therefore, we start with a simple but instructive case of unscreened Coulomb interaction between strictly 2D carriers, $V(r)=q_\delta q_\gamma/(4\pi K r)$, where $q_e=-e$, $q_h=e$, and K is the material permittivity. For such $V(r)$, Eq. (1) is analytically solvable,[32] and the exact scattering amplitude $f(\phi,g)$ can also be derived analytically.[32] The result is (in our notations)

$$f(\phi,g)=\frac{\Gamma(\frac{1}{2}-iG)}{\Gamma(iG)}\,\frac{\exp\left(2iG\ln\sin\frac{\phi}{2}\right)}{(ig)^{1/2}\sin\frac{\phi}{2}}, \tag{7}$$

$$G=\mu e^2/(4\pi K g\hbar^2). \tag{8}$$

We note that Eq. (7) is identical to the exact quantum result derived[32] for the scattering of a single 2D carrier by a Coulomb impurity, if in that result we replace the immobile impurity by a 2D carrier of initial velocity $\mathbf{v}_\delta$ and mass m_δ through a rigorous transformation[30] $v_\gamma\rightarrow|\mathbf{v}_\gamma-\mathbf{v}_\delta|$, $m_\gamma\rightarrow m_\gamma m_\delta/(m_\gamma+m_\delta)$, where v_γ and m_γ are the initial velocity and mass of the first carrier.

Using Eq. (7) and the Γ-function properties[33]

$$\Gamma(\tfrac{1}{2}+iG)\Gamma(\tfrac{1}{2}-iG)=\pi/\cosh(\pi G),$$

$$\Gamma(iG)\Gamma(-iG)=\pi/[G\sinh(\pi G)],$$

from Eq. (5) one obtains the exact differential cross section for distinguishable particles,

$$\sigma(\phi,g)=\frac{G}{g}\,\frac{\tanh(\pi G)}{\sin^2\frac{\phi}{2}}, \tag{9}$$

which is identical with the carrier-impurity cross section of Ref. 32 in the limit $m_\delta\rightarrow\infty$. Similarly, from Eq. (6) we obtain the exact cross section for indistinguishable particles,

$$\sigma(\phi,g)=\frac{G}{2g}\tanh(\pi G)\times\left\{\frac{1}{\sin^2\frac{\phi}{2}}+\frac{1}{\cos^2\frac{\phi}{2}}-\frac{\cos\left(2G\ln\left|\tan\frac{\phi}{2}\right|\right)}{\sin\frac{\phi}{2}\left|\cos\frac{\phi}{2}\right|}\right\}, \tag{10}$$

which is a 2D analogy of the Mott formula in three dimensions.[34] To our knowledge, Eq. (10) has not been published so far in the literature.

In the calculations we use the GaAs parameters $m_e=0.067m_0$, $m_h=0.44m_0$, and $K=10.9\epsilon_0$. For GaN we use $m_e=0.22m_0$, $m_h=1.98m_0$, and $K=5.5\epsilon_0$.[35]

Figure 1 compares function (10) with the function

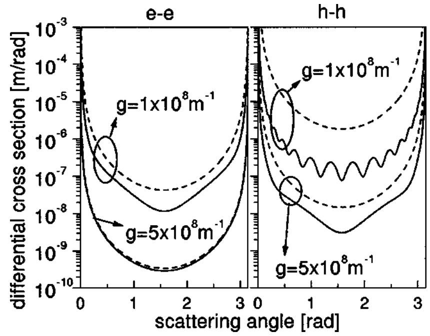

FIG. 1. Unscreened Coulomb cross section in dependence on the scattering angle ϕ for the 2D e-e and 2D h-h collisions in the GaAs quantum well. Full lines are the exact result (10), dashed lines the Born limit (11).

$$\sigma(\phi,g)=\frac{\pi G^2}{2g}\left\{\frac{1}{\sin^2\frac{\phi}{2}}+\frac{1}{\cos^2\frac{\phi}{2}}-\frac{1}{\sin\frac{\phi}{2}\left|\cos\frac{\phi}{2}\right|}\right\}, \tag{11}$$

which is the Born limit ($\pi G \ll 1$) of Eq. (10). Indeed, *the Born limit fails to fit the exact cross section*. Note also that the function $\cos[2G\ln|\tan(\phi/2)|]$ in the exchange term of Eq. (10) causes oscillations, nicely resolved in the exact h-h cross section for $g=10^8\ \mathrm{m}^{-1}$.

Now we ignore the particle indistinguishability and consider only Eq. (9). Equation (9) gives, in the Born limit,

$$\sigma_B(\phi,g)=\frac{\pi G^2}{g\sin^2\frac{\phi}{2}}, \tag{12}$$

while in the classical limit ($\pi G\gg 1$) it gives

$$\sigma_{cl}(\phi,g)=\frac{G}{g\sin^2\frac{\phi}{2}}. \tag{13}$$

Comparison of Eqs. (12) and (13) with the exact result (9) gives functions $\sigma_B/\sigma=G/\tanh(\pi G)$ and $\sigma_{cl}/\sigma=1/\tanh(\pi G)$, which no longer depend on ϕ. In Fig. 2 these fuctions are shown in dependence on g for e-e, e-h, and h-h collisions both in GaAs and GaN. Clearly, *the Born cross section fails to fit the exact cross section* ($\sigma_B/\sigma\rightarrow\infty$ for $g\rightarrow 0$), while the classical cross section works well ($\sigma_{cl}/\sigma\simeq 1$). This makes the 2D c-c collisions fundamentally different from the 3D c-c collisions, for which the purely Coulomb interaction gives[30] $\sigma=\sigma_B=\sigma_{cl}=(G/g)\sin^{-4}(\phi/2)$, i.e., *the Born approximation breakdown is inherent to two dimensions*. Due to the higher carrier effective mass and due to the lower permittivity, *in GaN the breakdown is much more pronounced*. The above conclusions, albeit proven for the unscreened interaction, are essentially also valid for the screened interaction, as we show in the next sections.

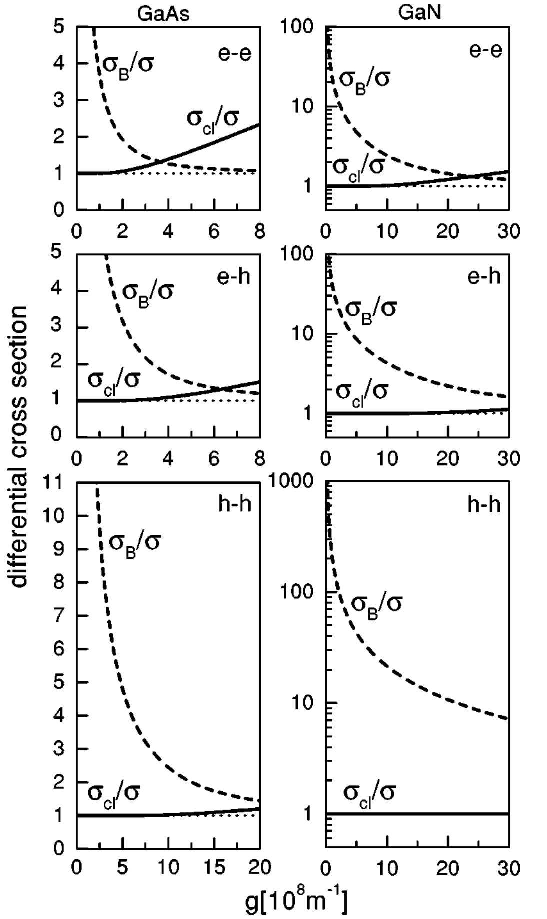

FIG. 2. Unscreened Coulomb cross sections in the Born limit [Eq. (12)] and in the classical limit [Eq. (13)] are compared with the exact cross section [Eq. (9)] in terms of σ_B/σ and σ_{cl}/σ. The results are provided for the 2D e-e, 2D e-h, and 2D h-h collisions in GaAs and GaN.

III. PHASE-SHIFT ANALYSIS

First we specify our screening model. We express the screened interaction as

$$V(r)=\frac{1}{(2\pi)^2}\int d\mathbf{Q}\, e^{i\mathbf{Qr}}\frac{q_\gamma q_\delta}{2KQ}\frac{F^{\gamma-\delta}(Q)}{\epsilon(Q)}, \tag{14}$$

where $q_\gamma q_\delta/2KQ$ is the Fourier transform of $q_\gamma q_\delta/4\pi K r$, $\epsilon(Q)$ is the screening function, and $F^{\gamma-\delta}(Q) =\int_{-\infty}^{\infty}dz\int_{-\infty}^{\infty}dz_0\ \chi_\gamma^2(z)e^{-Q|z-z_0|}\chi_\delta^2(z_0)$ is the form factor which accounts for the finite thickness of the 2D plasma. Equation (14) with $\epsilon(Q)=1$ can easily be derived from Eq. (3) with $W(r,z-z_0)=q_\gamma q_\delta/[4\pi K\sqrt{r^2+(z-z_0)^2}]$, while Eq. (14) with screening is a standard result of the RPA theory,[9,36] applied to a 2D system [37] in the limit of static screening. For a strictly 2D system[38] $\epsilon(Q)=1+Q_{SC}/Q$, where Q_{SC} is the inverse screening length. The strictly 2D form can be modified to the quasi-2D form[18]

$$\epsilon(Q)=1+Q_{SC}F(Q)/Q, \tag{15}$$

strictly valid in case that $\chi_e(z)=\chi_h(z)$.[39] In this paper we use the screening function (15) and evaluate $F(Q)$ assuming $\chi_e=\chi_h=\sqrt{2/L}\sin(\pi z/L)$, where L is the quantum-well width [for $\chi_e=\chi_h$, the indices γ,δ in the form factor $F(Q)$ can be omitted]. This screening model has already been found to be reasonable in some experimental situations,[40] and in our case allows a transparent presentation of the phase-shift analysis. In the calculations we use $L=10$ nm, but we note that our results are not very sensitive to the choice of L or even to the choice of χ_e and χ_h, if the choice is reasonable.

Applications of the phase shift analysis to the 3D and 2D scattering on a fixed scattering center can be found, e.g., in Refs. 30, 32 and 41. Below we present the application to 2D c-c scattering, give a number of details necessary for a successfull implementation, and show representative numerical results for the phase shifts.

One can use the partial wave (P_m) expansion

$$\Phi(r,\phi)=\sum_{m=-\infty}^{\infty}c_m\frac{1}{\sqrt{r}}P_m(r)e^{im\phi} \tag{16}$$

to transform Eq. (1) into a set of radial equations

$$\left[\frac{\partial^2}{\partial r^2}-\frac{\mu}{\hbar^2}V(r)-\frac{(m^2-1/4)}{r^2}+\left(\frac{g}{2}\right)^2\right]P_m(r)=0,$$
$$m=0,\pm1,\pm2,\ldots. \tag{17}$$

For $r\to0$, Eq. (17) takes the form

$$\left[\frac{\partial^2}{\partial r^2}-\frac{(m^2-1/4)}{r^2}\right]P_m(r)=0, \tag{18}$$

the solution of which is

$$P_m(r\to0)\propto\sqrt{r}r^{|m|}. \tag{19}$$

This gives the boundary condition $P_m(0)=0$, which, with the Eq. (17), determines $P_m(r)$ except for a multiplication constant. At $r\to\infty$, Eq. (17) reduces to $[\partial^2/\partial r^2+(g/2)^2]P_m(r)=0$. We thus obtain $P_m(r\to\infty)\propto\cos[(g/2)r+X_m]$, where the phase X_m is fixed by exact solution of Eq. (17). If we define $X_m=-(\pi/2)m-(\pi/4)+\delta_m$, we can write the asymptotic solution of Eq. (17) as

$$P_m(r\to\infty)=\sqrt{\frac{4}{\pi g}}\cos\left(\frac{g}{2}r-\frac{\pi}{2}m-\frac{\pi}{4}+\delta_m\right). \tag{20}$$

Here δ_m is the phase shift caused by $V(r)$, and the multiplication constant $\sqrt{4/\pi g}$ is discussed later on.

The 2D c-c collision cross section as a function of δ_m can be expressed through exact quantum formulas [Eqs. (33) and (34)]. Thus, once δ_m is known, the problem is completely solved. δ_m can in principle be evaluated by tailoring the exact (numerical) solution of Eq. (17) with the asymptotic form (20). In practice, however, this does not give a stable (r-independent) δ_m, because numerically one only works with finite r rather than with $r\to\infty$. Now we show how to obtain a stable and accurate δ_m.

We need asymptotic solution of Eq. (17) for large but finite $r\gg Q_{SC}^{-1}$. For such r the decrease of $V(r)$ is faster than r^{-2} (Ref. 32), so that at large enough r Eq. (17) reduces to the equation

$$\left[\frac{\partial^2}{\partial r^2}-\frac{(m^2-1/4)}{r^2}+\left(\frac{g}{2}\right)^2\right]P_m(r)=0, \tag{21}$$

with independent solutions $P_m(r)=\sqrt{r}J_m[(g/2)r]$ and $P_m(r)=\sqrt{r}Y_m[(g/2)r]$,[33] where J_m and Y_m are the cylindrical Bessel functions.[42] The desired asymptotic solution is their linear combination in the form

$$P_m(r)=\sqrt{r}\left[J_m\left(\frac{g}{2}r\right)\cos\delta_m - Y_m\left(\frac{g}{2}r\right)\sin\delta_m\right], \quad r\gg Q_{SC}^{-1}, \tag{22}$$

which in the limit $r\to\infty$ reduces[43] to formula (20) including the factor $\sqrt{4/\pi g}$.

Let $P_m(r)_{\rm NUM}$ stand for the numerical solution of Eq. (17). Equation (22) can be tailored with $P_m(r)_{\rm NUM}$ as

$$\frac{P_m'(r)}{P_m(r)}=\frac{P_m'(r)_{\rm NUM}}{P_m(r)_{\rm NUM}}. \tag{23}$$

From Eqs. (23) and (22) we obtain

$$\tan(\delta_m)=\frac{J_m'\left(\frac{g}{2}r\right)-\gamma(r)J_m\left(\frac{g}{2}r\right)}{Y_m'\left(\frac{g}{2}r\right)-\gamma(r)Y_m\left(\frac{g}{2}r\right)}, \tag{24}$$

where

$$\gamma(r)=\frac{P_m'(r)_{\rm NUM}}{P_m(r)_{\rm NUM}}-(2r)^{-1}. \tag{25}$$

Finally, to evaluate $P_m(r)_{\rm NUM}$ we solve Eq. (17) using the finite-difference scheme

$$P_m(r_j)=2P_m(r_{j-1})-P_m(r_{j-2})+\Delta r^2 P_m''(r_{j-1}), \tag{26}$$

where $r_j=j\cdot\Delta r$ and P_m'' is given by Eqs. (17). Although the scheme works for $j=2,3,\ldots,$ it is practical to start with a much larger j than 2. If we choose j such that r_j still obeys the inequality $|(m^2-1/4)/r^2|\gg|(g/2)^2-\mu V(r)/\hbar^2|$, then Eq. (18) is still a good alternative of Eq. (17) and we can initialize $P_m(r_{j-1})$ and $P_m(r_{j-2})$ using Eq. (19). The resulting $P_m(r)_{\rm NUM}$ and Eq. (24) give a stable (r-independent) δ_m for $r\gg Q_{SC}^{-1}$.

The described procedure is exact but rather slow. Therefore, we also introduce a highly accurate and fast working approximation. We first show that the exact phase shifts converge for $m^2\gg 1/4$ toward the quasiclassical limit

$$\delta_m^{clas}=\int_{r_a}^{\infty}dr\ \sqrt{\left(\frac{g}{2}\right)^2-\frac{\mu V(r)}{\hbar^2}-\frac{m^2}{r^2}} - \int_{r_b}^{\infty}dr\ \sqrt{\left(\frac{g}{2}\right)^2-\frac{m^2}{r^2}}, \tag{27}$$

where r_a and r_b are the r values at which the first and second integrands, respectively, are zero.

The solution of Eq. (17) in the quasiclassical limit is[30]

$$P_m(r)\propto\frac{1}{\sqrt{p(r)}}\cos\left(\int_{r_a}^{r}dr\,p(r)-\frac{\pi}{4}\right), \quad r>r_a, \tag{28}$$

where $p(r)=\sqrt{(g/2)^2-\mu V(r)/\hbar^2-(m^2-1/4)/r^2}$. For $m\gg 1/4$ we can replace $m^2-1/4$ by m^2 [Eq. (28), for $V(r)=0$ and $r\to\infty$, then gives the asymptotic form of Eq. (20) with $\delta_m=0$]. The phase shift (27) is the phase difference of the wave function (28) and of the same wave function with $V(r)=0$, both taken in the limit $r\to\infty$. Equation (27) is a 2D analog of the known 3D result.[30]

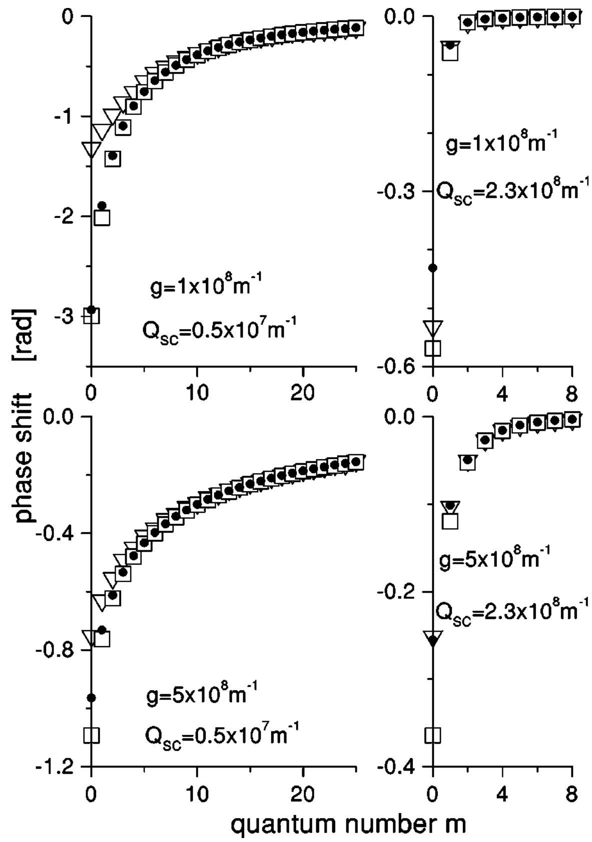

FIG. 3. Phase shift δ_m as a function of m for the e-e collision at various wave vectors (g) and various screening lengths (Q_{SC}). Full circles show the exact phase shifts, open squares the quasiclassical phase shifts (δ_m^{clas}), and open triangles the Born phase shifts (δ_m^{Born}), all for the GaAs quantum well.

Let us compare the quasiclassical phase shifts with the exact ones. The output of the exact phase-shift analysis [Eq. (24)] is $\tan\delta_m$, which gives δ_m as

$$\delta_m=\arctan(\tan\delta_m)+j\pi, \tag{29}$$

where j is an arbitrary integer. The quasiclassical limit (27) directly gives δ_m^{clas}, so if one writes

$$\delta_m^{clas}=\arctan(\tan\delta_m^{clas})+l\pi, \tag{30}$$

then Eq. (30) defines the integer l. Since $\delta_m\to\delta_m^{clas}$ for $m^2\gg 1/4$, comparison of Eq. (29) and (30) gives $j=l$.

In Fig. 3 we compare δ_m and δ_m^{clas} for the e-e collisions at various g and Q_{SC}. *When $m^2\gg 1/4$, the exact phase shifts are perfectly fitted by the quasiclassical ones for any g and Q_{SC}. This proves that both computational programs work well* and shows that the exact analysis is only needed say for $|m|=0,1,2,3$, while for $|m|>3$ the quasiclassical formula (27) is sufficient with a high accuracy. The use of Eq. (27) decreases the computational time per one phase typically 10–50 times. The phase shifts for the h-h scattering (not

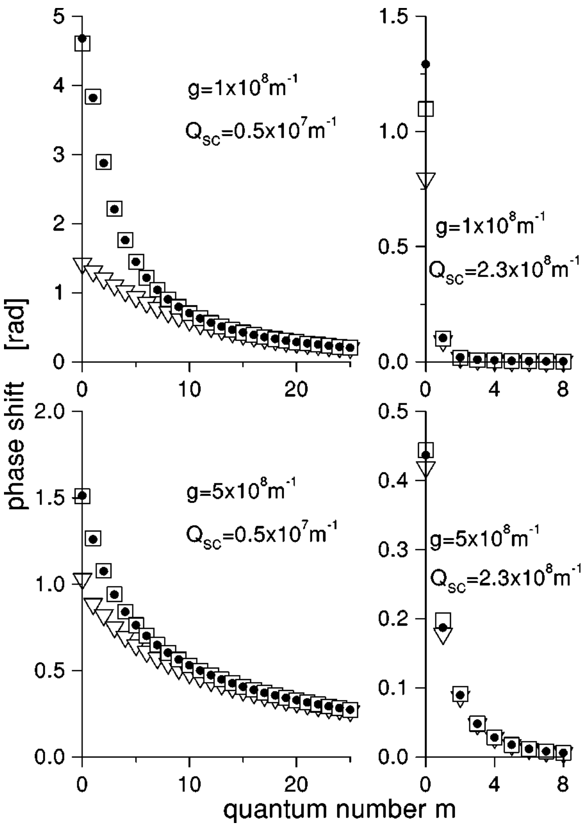

FIG. 4. The same as in Fig. 3, but for the e-h collision.

shown) behave similarly, while for the e-h collisions (see Fig. 4) the only change is that the phase shifts are positive.

Figures 3 and 4 also show phase shifts in the Born limit:[30,41]

$$\delta_m^{Born}=\arctan\left\{-\frac{\pi}{2}\int_0^\infty dr\, rJ_m^2\left(\frac{g}{2}r\right)\frac{\mu}{\hbar^2}V(r)\right\}. \quad (31)$$

The Born phase shifts fit the exact phase shifts only for large g and Q_{SC}, so their applicability[32] is not general.

IV. CROSS SECTION OF SCREENED 2D c-c COLLISION: EXACT VERSUS BORN

Once δ_m is known, the exact 2D c-c scattering cross section can be generated. First we express through δ_m the scattering amplitude $f(\phi,g)$. It reads

$$f(\phi,g)=\sqrt{\frac{4i}{\pi g}}\sum_{m=-\infty}^{\infty}e^{im\phi}e^{i\delta_m}\sin\delta_m. \quad (32)$$

Equation (32) can be derived[30] by comparing Eq. (4) and (16) at $r\to\infty$. Then $P_m(r)$ in Eq. (16) is given by Eq. (20), and if we use the identity (valid for $r\to\infty$)

$$\exp\left(i\frac{\mathbf{g}}{2}\mathbf{r}\right)=\sqrt{\frac{4}{\pi g r}}\sum_{m=-\infty}^{\infty}i^m e^{im\phi}\cos\left(\frac{g}{2}r-\frac{\pi}{2}m-\frac{\pi}{4}\right),$$

we can express the difference $\phi(r,\phi)-\exp[i(\mathbf{g}/2)\mathbf{r}]$ as a sum of the term proportional to $r^{-1/2}\exp[i(g/2)r]$ and the term proportional to $r^{-1/2}\exp[-i(g/2)r]$. The latter term is not physical ($r^{-1/2}\exp[-i(g/2)r]$ is a circular wave running toward the scattering center) and disappears only if c_m in Eq. (16) is chosen as $\exp(i[(\pi/2)m+\delta_m])$. Then only the term $f(\phi,g)r^{-1/2}\exp[i(g/2)r]$ remains, with $f(\phi,g)$ given by Eq. (32).

Using Eq. (32) from Eq. (5) one obtains the exact differential scattering cross section

$$\sigma(\phi,g)=\frac{4}{\pi g}\left\{\left[\sum_{m=-\infty}^{\infty}\sin\delta_m\cos(\delta_m+m\phi)\right]^2+\left[\sum_{m=-\infty}^{\infty}\sin\delta_m\sin(\delta_m+m\phi)\right]^2\right\}, \quad (33)$$

valid for distinguishable particles. Similarly, for indistinguishable particles, from Eq. (6) we easily obtain

$$\begin{aligned}\sigma(\phi,g)=&\frac{2}{\pi g}\left\{\left[\sum_{m=-\infty}^{\infty}\sin\delta_m\cos(\delta_m+m\phi)\right]^2+\left[\sum_{m=-\infty}^{\infty}\sin\delta_m\sin(\delta_m+m\phi)\right]^2\right\}\\&+\frac{2}{\pi g}\left\{\left[\sum_{m=-\infty}^{\infty}\sin\delta_m\cos(\delta_m+m\phi+m\pi)\right]^2+\left[\sum_{m=-\infty}^{\infty}\sin\delta_m\sin(\delta_m+m\phi+m\pi)\right]^2\right\}\\&-\frac{2}{\pi g}\sum_{m=-\infty}^{\infty}\sum_{m'=-\infty}^{\infty}\sin\delta_m\sin\delta_{m'}\\&\times\cos(\delta_m-\delta_{m'}+m\phi-m'\phi-m'\pi),\end{aligned} \quad (34)$$

where the third term is due to the exchange effect.

Our aim is to compare Eqs. (33) and (34) with their Born limit. The Born cross section (σ_B) was derived in our previous work[18] from the Fermi golden rule. The result is

$$\sigma_B(\phi,g)=\pi G^2 g\frac{F(Q)^2}{Q^2\epsilon(Q)^2} \quad (35)$$

for distinguishable particles, and

$$\sigma_B(\phi,g)=\pi G^2 g\frac{1}{2}\left[\frac{F(Q)^2}{Q^2\epsilon(Q)^2}+\frac{F(Q')^2}{Q'^2\epsilon(Q')^2}-\frac{F(Q)F(Q')}{Q\epsilon(Q)Q'\epsilon(Q')}\right] \quad (36)$$

for indistinguishable particles, where $Q=g\sin(\phi/2)$, $Q'=g|\cos(\phi/2)|$, and G is given by Eq. (8). As expected, for $F(Q)=1$ and $\epsilon(Q)=1$, Eqs. (35) and (36) give the unscreened Born results (12) and (11).

We note that the Born cross sections (35) and (36) can also be derived directly from the exact cross sections (33) and (34). The derivation is similar to that one for a fixed scattering center,[30,32] so we only mention basic steps. First one assumes that $V(r)$ is a small perturbation, and obtains[32] the Born phase shifts (31). Second, one simplifies Eqs. (33), (34), and (31), assuming that all phase shifts are small.[30,32] Third, using Eq. (31), the relation[33] $\sum_{m=-\infty}^{\infty}J_m^2[(g/2)r]e^{im\phi}$

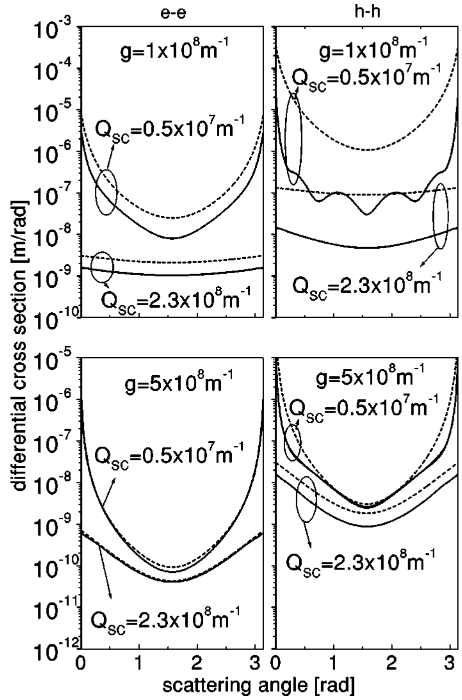

FIG. 5. Differential scattering cross section vs scattering angle for the 2D e-e and 2D h-h collisions. The wave vectors (g) and screening lengths (Q_{SC}) used in the calculations are indicated. The exact cross section (34) is shown by a full line, the Born cross section (36) by a dashed line.

$=J_0[(g/2)r\sin(\phi/2]$, and Eq. (14), from Eqs. (33) and (34) one obtains Eqs. (35) and (36).

Figure 5 compares the exact and Born cross sections for the e-e and h-h collisions in the GaAs quantum well at various Q_{SC} and g [$Q_{SC}=2.3\times10^8$ m^{-1} is the highest electronic screening in the GaAs quantum well—the Thomas-Fermi screening $Q_{SC}=e^2m_e/(2\pi K\hbar^2)$]. As in Fig. 1, in Fig. 5 *the Born limit also fails to fit the exact result*. One also sees the oscillations due to the exchange effect (cf. Fig. 1) in the exact h-h cross section for $g=10^8$ m^{-1} and $Q_{SC}=0.5\times10^7$ m^{-1}.

In Fig. 6 we show the same result as in Fig. 5, but for e-h scattering, i.e., we evaluate the exact and Born cross sections from formulas (33) and (35). The Born limit again overestimates the exact result and, unlike the Born limit, the exact result is sensitive to the sign of the intercarrier interaction, which we demonstrate by changing the attractive interaction to a repulsive one. *For $Q_{SC}=0$ the phase-shift analysis gives the same numerical results (Figs. 1 and 2) as do the analytical cross sections (9) and (10), but one has to apply a more sophisticated procedure,[44] appropriate for bare Coulomb scattering.*

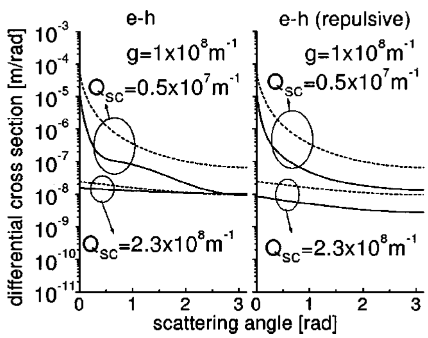

FIG. 6. The same as in Fig. 5, but for e-h collisions. Also shown are results for the repulsive e-h interaction.

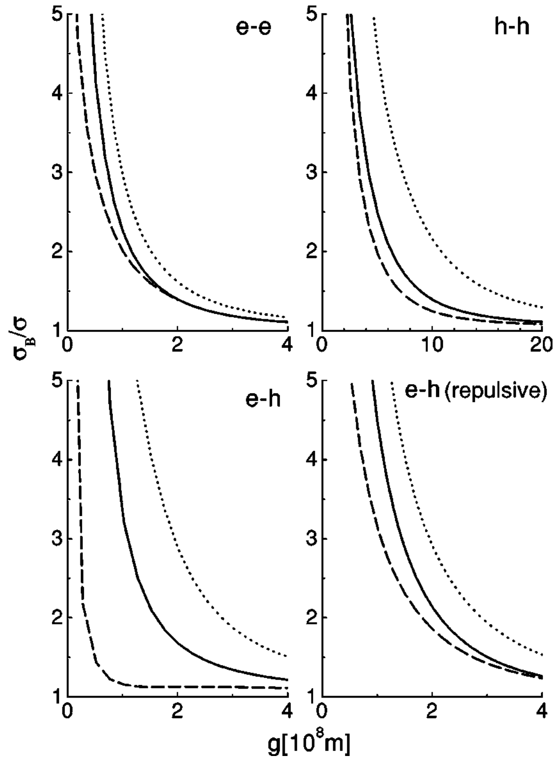

FIG. 7. Cross-section ratio $\sigma_B(g)/\sigma(g)$ versus the relative wave vector g for the e-e, e-h, and h-h collisions in the GaAs quantum well. Here $\sigma(g)$ is the exact total cross section, and $\sigma_B(g)$ is the Born total cross section. The full, dashed, and dotted lines show the results for $Q_{SC}=0.5\times10^7$, 8×10^7, and 2.3×10^8 m^{-1}, respectively. Also shown are results for the repulsive e-h interaction.

Finally, we evaluate the total scattering cross section

$$\sigma(g)=\int_0^{2\pi}d\phi\,\sigma(\phi,g). \tag{37}$$

Inserting Eq. (33) for $\sigma(\phi,g)$ one obtains the exact total cross section for distinguishable particles:

$$\sigma(g)=\frac{8}{g}\sum_{m=-\infty}^{\infty}\sin^2\delta_m. \tag{38}$$

Similarly, for indistinguishable particles, we easily obtain

$$\sigma(g)=\frac{8}{g}\sum_{m=-\infty}^{\infty}\sin^2\delta_m-\frac{4}{g}\sum_{m=-\infty}^{\infty}\sin^2\delta_m\cos(m\pi). \tag{39}$$

The corresponding Born total cross sections can be evaluated by inserting Eqs. (35) and (36) into Eq. (37).

In Fig. 7 the Born total cross section $\sigma_B(g)$ is compared with the exact total cross section $\sigma(g)$ in terms of the ratio $\sigma_B(g)/\sigma(g)$. The results are calculated for e-e, e-h, and h-h collisions in the GaAs quantum well at various levels of screening. Note that the screened σ_B/σ curves are similar to the unscreened results in Fig. 2, *except that the screening* *weakens the Born approximation breakdown. The Born approximation still overestimates the exact cross section in a broad range of carrier energies and screening lengths.* In case of the e-h interaction one sees that its attractive character reduces the difference between $\sigma(g)$ and $\sigma_B(g)$ at large Q_{SC}. At small Q_{SC}, $\sigma(g)$ is no longer sensitive to the sign of the interaction.

Similar results (not shown) were obtained also for the GaN quantum well. The only difference was a more pronounced failure of the Born approximation, already envisioned in Fig. 2.

For completeness, in the Appendix we examine the screened 2D c-c collision as a classical event. We show that the classical treatment fits almost perfectly the exact treatment if the screening is weak.

V. 2D *c-c* SCATTERING RATE

The 2D c-c collision rate reads

$$\Gamma^{out}_{\gamma-\delta}(\mathbf{k})=2\sum_{\mathbf{k}_0} f_\delta(\mathbf{k}_0)\frac{\hbar g}{\mu}\int_0^{2\pi}d\phi\,\sigma^{\gamma-\delta}(\phi,g)[1-f_\gamma(\mathbf{k}')]\times[1-f_\delta(\mathbf{k}_0')], \tag{40}$$

where $\gamma=e,h$ and $\delta=e,h$, $f_e(\mathbf{k})$ and $f_h(\mathbf{k})$ are the electron and hole distribution functions, and the states $\mathbf{k}'$ and $\mathbf{k}_0'$ as functions of ϕ, $\mathbf{k}$, and $\mathbf{k}_0$ are fixed by the conservation of energy and momentum.

If one inserts the Born cross section [Eqs. (35) and (36)], for $\sigma(\phi,g)$, then formula (40) represents the Born 2D c-c scattering rate as can be derived from the Fermi golden rule. If we insert the exact quantum cross section [Eqs. (33) and (34)] for $\sigma(\phi,g)$, then Eq. (40) provides us with the exact (in Markovian limit) 2D c-c scattering rate. It should also be derivable from the first-principles non-Markovian kinetics valid in all orders in the intercarrier interaction (see Appendix XIII in Ref. 45).

The static screening length Q_{SC} has so far been a parameter. In the following we use[18]

$$Q_{SC}=\frac{e^2}{2\pi K\hbar^2}[m_e f_e(0)+m_h f_h(0)] \tag{41}$$

for the h-h collisions, while in case of the e-e and e-h collisions we omit the screening by holes and take

$$Q_{SC}=\frac{e^2}{2\pi K\hbar^2}m_e f_e(0). \tag{42}$$

Equation (42) roughly incorporates the fact that in a dynamic screening model the heavy holes would be too slow to follow the fast electronic motion. For this study the static screening is sufficient, because once we find a difference between the Born and exact results for static screening, we expect an even larger difference for the dynamic screening: The dynamic screening is weaker than the static one,[20,15,17] and *our results show that the weaker the screening the worse the Born approximation in two dimensions (see, e.g., Fig. 7 for* $Q_{SC}>0$ *and Fig. 2 for* $Q_{SC}=0$).

First we study the 2D c-c scattering rate in a high-density e-h plasma, as typically encountered in semiconductor-

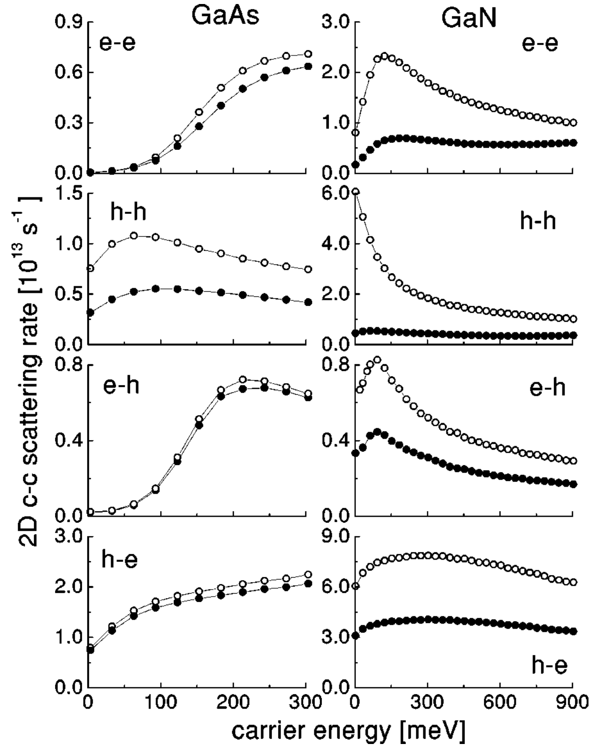

FIG. 8. 2D carrier-carrier scattering rate Γ^{out} (e-e, h-h, e-h, and h-e) as a function of the carrier energy, calculated for the equilibrium 2D e-h plasma at temperature 300 K and an e-h pair density of 4×10^{12} cm^{-2}. The left column shows the results for the GaAs quantum well, and the right column the results for the GaN quantum well. Full circles are the exact results, open circles are the Born results.

quantum-well lasers:[8,46] We approximate the distributions $f_e(\mathbf{k})$ and $f_h(\mathbf{k})$ as the equilibrium Fermi distributions at temperature $T=300$ K and carrier density $n_e=n_h=4\times10^{12}$ cm^{-2}.

Figure 8 shows the calculated 2D c-c scattering rates. *In the GaN quantum well the Born approximation overestimates exact results for e-e and h-h scattering by almost one order of magnitude*. In the GaAs quantum well it works better, but a remarkable overestimation is still seen for the h-h scattering. The overestimation is systematically lower for the e-h and h-e scattering, which we already saw in Fig. 7 for strong screening.

Now we calculate the 2D c-c scattering rate under conditions typical for time-resolved optical spectroscopy. In that kind of experiment a nonthermal 2D e-h plasma is excited in the quantum well by a fast quasimonoenergetic laser pulse, and the time-resolved absorption spectrum is measured in order to detect the 2D c-c scattering.[6] Interpretation of such experiments[18,38] is not the aim of this paper, we just wish to test the applicability of the Born approximation.

The initial energy distribution of the photoexcited plasma roughly follows the energy spectrum of the pump pulse. Assuming a Gaussian pulse spectrum centered at excess energy W with a halfwidth ΔW, we obtain[17]

$$f_e(\mathbf{k})\propto\exp\left\{-\left(\frac{\hbar^2k^2}{2m_e}-W_e\right)^2\Big/\,2\Delta W_e^2\right\}, \tag{43}$$

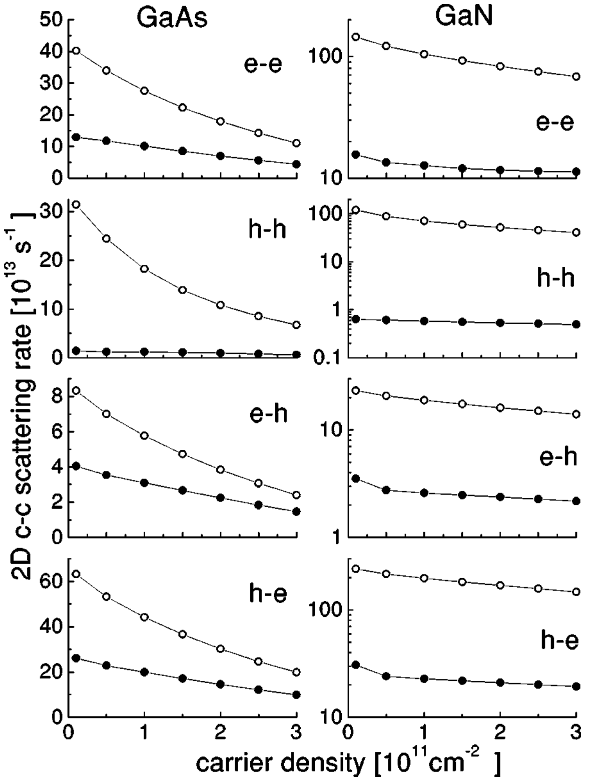

FIG. 9. 2D carrier-carrier scattering rate Γ^{out} (e-e, h-h, e-h, and h-e) as a function of the e-h pair density. In the calculation, the nonthermal 2D e-h plasma with a Gaussian carrier energy distribution [Eqs. (43) and (44)] was considered, and the 2D c-c scattering rate was evaluated for a carrier with energy just in the center of the distribution ($W_e=17.2$ meV and $W_h=2.8$ meV for the GaAs, and $W_e=18$ meV and $W_h=2$ meV for GaN). Results for the GaAs (GaN) quantum well are in the left (right) column. Full circles are the exact results, open circles the Born results.

$$f_h(\mathbf{k}) \propto \exp\left\{ -\left(\frac{\hbar^2 k^2}{2m_h} - W_h\right)^2 \Big/ 2\Delta W_h^2 \right\}, \qquad (44)$$

where $W_e = m_h W/(m_e+m_h)$, $W_h = m_e W/(m_e+m_h)$, etc. for $\Delta W_{e,h}$. We insert the above distributions into the 2D c-c scattering rate (40) and evaluate it for a carrier energy in the center of the distribution in order to assess the characteristic scattering rate.[17] Results are presented in Fig. 9 as function of the carrier density for $W = 2\Delta W = 20$ meV. The Born approximation overestimates the exact 2D c-c scattering rate far more than in Fig. 8, because the screening is much weaker owing to the nonthermal distribution and to the lower plasma density. *The overestimation by a factor of 10–100 in the GaN corresponds to the analytical results of Fig. 2.*

VI. SUMMARY AND COMPARISON WITH PREVIOUS WORK

In summary, in this paper Markovian 2D c-c scattering has been studied by means of phase-shift analysis. The output of the analysis shows exact quantum results for the 2D c-c scattering cross section and 2D c-c scattering rate. We have compared these results with the Born approximation. We have demonstrated, for GaAs and GaN quantum-well systems, that the Born approximation can grossly overestimate the exact 2D c-c scattering cross section and the exact 2D c-c scattering rate. The overestimation by a factor of 2–100 has been found under conditions typical for semiconductor-quantum-well lasers, and especially under conditions typical for the ultrafast excite-probe spectroscopy. We have identified the carrier two dimensionality as a main reason for the Born approximation breakdown, we believe that in 3D systems the Born approximation works better. Major conclusions have been supported by analytical calculations (Sec. II), which can easy be verified. Finally, a detailed algorithm of the phase-shift analysis (Sec. III.) has been provided for potential users, and a classical 2D c-c collision analysis (see the Appendix) has been proposed as an alternative approach, appropriate for the weak screening limit.

Our study has been performed in the Markovian c-c scattering limit, so a few remarks should be added concerning the non-Markovian c-c scattering theory previously derived[45] and applied by several groups in 3D GaAs systems.[45,47–51] Due to its complexity, the non-Markovian theory was also formulated in the Born approximation.[45] Therefore, a formal derivation of the Markovian c-c scattering limit (Markovian Boltzmann equation) from such non-Markovian theory gives a conventional ‘‘Born-approximation-based’’ Markovian c-c scattering,[45,52] the 2D version of which we criticize in this paper. Owing to our criticism, several problems emerge. First, in case of 2D systems, the non-Markovian theory relying on the Born approximation[45,47–51] should be generalized for a c-c scattering of arbitrary strength, because once the Born c-c scattering fails in the Markovian limit, then its validity is also questionable in the non-Markovian theory (the question of how to avoid the Born approximation in non-Markovian theory is addressed in Appendix XIII of Ref. 45). Further, it would be useful to derive the Markovian 2D c-c scattering rate with the exact c-c cross section [Eq. (40) with exact $\sigma(\phi,g)$] directly from such generalized non-Markovian theory in order to give a systematic formal support to our *ad hoc* formulation. These problems are beyond the scope of this paper, and we are not aware of any non-Markovian analysis of 2D c-c scattering in the literature. 3D analysis[50] shows that non-Markovian memory effects can modify the Markovian c-c scattering, if ultrafast carrier relaxation is considered. However, these modifications, although not negligible,[50] are not so pronounced as the order-of-magnitude changes introduced by our phase-shift analysis. If the same holds in the 2D systems (we consider it to be very likely, albeit presently we cannot give a rigorous proof), then a major problem of the 2D c-c scattering theory is not the Markovian approximation but the Born approximation.

The main limitations of our Markovian model are the following. We have considered 2D c-c scattering only in the lowest-energy subband. A complete phase-shift analysis of a multisubband system would be too difficult, but a reasonable compromise might be a phase-shift analysis of intrasubband c-c collisions combined with the Born approximation for intersubband c-c collisions. Further, beyond the scope of this paper is Friedel's sum rule correction of the scattering potential entering the phase-shift analysis.[32,41] We prefered potential (14) in order to present a transparent introductory comparison of the exact and Born calculations.

We conclude by mentioning previous work relevant to our results. References 18 and 26 in fact also presented 2D c-c scattering analyses valid in all orders in the intercarrier interaction, because, although fully classical, these analyses were performed under conditions where the classical and exact quantum cross sections coincide (see also the Appendix of this paper). In Refs. 18 and 26 the failure of the Born 2D c-c scattering model was proven in the weak screening limit. More recently, the authors of Ref. 53 analyzed the 2D quasiparticle life time in the limit of low temperature and low excitation energy. In that limit they summed up all orders of the intercarrier interaction by means of the diagramatic technique, and also found results differing from the Born approximation.

For 3D c-c scattering, a correction due to the phase shifts was presented in the Appendix A of Ref. 7. The correction is acomplished by scaling the Born 3D c-c scattering cross section by the factor $h=\sigma_T/\sigma_T^B$ (taken from Ref. 41), where σ_T and σ_T^B are the total momentum-transfer cross sections calculated by the phase-shift method and by the Born approximation, respectively [see Eqs. (A1) and (A12) in that appendix]. We believe that with regards to its definition the factor h can correctly scale only the momentum-transfer cross section but not the scattering cross section. Further, in Ref. 7 only the total scattering cross section is scaled, but the differential scattering cross section (the angle distribution) still remains in the Born approximation.

Finally, the author of Ref. 54 calculated 3D c-c scattering in metals by evaluating the lowest phase shift. Unfortunately, such an approach is not applicable in the semiconductor-quantum-well systems considered by us, as we often need to evaluate 100–1000 phase shifts.

ACKNOWLEDGMENTS

M.M. greatly acknowledges the support from the J.W. Fulbright Commision and from the University of Illinois at Urbana during his stay at the Beckmann Institute, where a part of this work was done. A.M. and M.M. were also supported by the Grant Agency of the Slovak Academy of Sciences, Contract No. 2/4057/97. Special thanks go to Professor Karl Hess for numerous important discussions concerning this work, and for his kind hospitality at the Beckmann Institute.

APPENDIX: SCREENED 2D C-C COLLISION AS A CLASSICAL EVENT

In Sec. II we derived the hierarchy of exact, Born, and classical cross sections analytically for a bare Coulomb potential, and pointed out that the classical description is an excellent approximation just when the Born approximation breakdown becomes most pronounced. In this appendix we analyze the classical 2D c-c collision in the presence of screening, and we show that the classical picture still works well if the screening is weak.

In a classical 2D c-c collision, the scattering angle ϕ is fully determined by Newton equations of motion, if the relative wave vector $\mathbf{g}$ and the impact distance b of the colliding carriers are known. The result is[30,55]

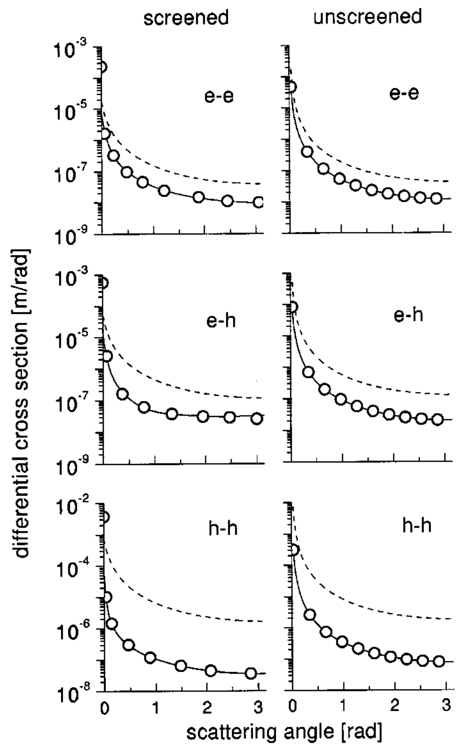

FIG. 10. Differential cross sections of the e-e, e-h, and h-h collisions in the GaAs quantum well. The left (right) column of figures shows the cross sections obtained for screened (unscreened) intercarrier interaction, solid lines show the exact cross section, dashed lines show the Born cross section, and open circles show the classical cross section. For a convenient comparison of quantum and classical cross sections, we ignore the quantum particle indistinguishability, the relative wave vector used in the calculations is $g=10^8$ m^{-1}; the screening is given by $Q_{SC}=0.5\times10^7$ m^{-1}.

$$\pm\phi=\pi-2\int_{r_{min}}^{\infty}dr\,\frac{b}{r^2\left\{1-\left(\frac{b}{r}\right)^2-\frac{4\mu V(r)}{\hbar^2g^2}\right\}^{1/2}},\quad\text{(A1)}$$

where the plus and minus signs on the left-hand side hold for the attractive and repulsive interactions, respectively, and r_{min} is the minimum intercarrier distance—the solution of the equation

$$1-\left(\frac{b}{r}\right)^2-\frac{4\mu V(r)}{\hbar^2g^2}=0.\quad\text{(A2)}$$

We note that Eqs. (A1) and (A2) hold also for the 3D collisions (for which they are usually presented[55,30]), because in the classical picture the 3D collision can be viewed as a 2D collision in the plane defined by trajectories of the colliding 3D carriers. For the 2D collision (but not for three dimensional) the classical differential cross section is defined as

$$\sigma_{cl}(\phi,g)=\left|\frac{db}{d\phi}\right|.\quad\text{(A3)}$$

For $V(r)=q_\gamma q_\delta/(4\pi Kr)$ Eqs. (A1), (A2), and (A3) give analytical result (13), originally derived as a clasical limit of the quantum result (9). For a screened $V(r)$, Eqs. (A1)–(A3) have to be solved numerically.

Equation (A1) can also be derived as a classical limit of the phase-shift analysis. The derivation is similar to the corresponding 3D derivation,[30] so we only give a brief outline. Using $\Sigma_{m=-\infty}^{\infty} e^{im\phi} = 2\pi\delta(\phi)$, we rewrite the scattering amplitude (32) for $\phi \neq 0$ as

$$f(\phi,g) = \sqrt{\frac{4i}{\pi g}} \sum_{m=-\infty}^{\infty} e^{i(m\phi + 2\delta_m)}. \tag{A4}$$

In the classical limit the phase shifts are expected to be large. Therefore, $e^{i(m\phi+2\delta_m)}$ exhibits fast oscillations as a function of m, and most of the terms in sum (A4) cancel mutually. Only those terms for which either $m\phi + 2\delta_m$ or $-m\phi + 2\delta_m$ approaches its maximum do not cancel. This is the case for m obeying the equation

$$\frac{d}{dm}(2\delta_m \pm m\phi) = 0. \tag{A5}$$

From Eq. (A5) we obtain Eq. (A1), after substituting the quasiclassical phase shift (27) for δ_m: One has to evaluate $d\delta_m/dm$, keeping in mind that in Eq. (27) r_a and r_b depend on m, and in the final result one has to replace the quantity $\hbar m$ by its classical counterpart $\hbar g b$.

In Fig. 10 we compare the hierarchy of exact, Born, and classical cross sections derived for $V(r) = q_\gamma q_\delta/(4\pi K r)$ [formulas (9), (12), and (13)] with the same hierarchy evaluated for a screened strictly 2D $V(r)$. In both cases we ignore the quantum particle indistinguishability for a convenient comparison of quantum and classical results; numerical results are provided for $Q_{sc} = 0.5 \times 10^7$ m^{-1} and $g = 10^8$ m^{-1}. One can see that the classical result also fits the exact result very well in the screened case. The exceptions are the scattering angles $\phi \to 0$, for which the classical cross section also diverges.

This divergency deserves a comment. The quantum cross section diverges at $\phi \to 0$ only if $V(r) \propto r^{-1}$, while the classical cross section diverges at $\phi \to 0$ for screened $V(r)$. This is due to the fact that the classical particles are scattered to a zero scattering angle only if the force between them is zero, which is the case only for an infinite impact distance. This divergency implies, of course, that the classical two-body collision rate [Eq. (40), with $\sigma(\phi,g)$ taken in the classical limit] also diverges; however, it is worth mentioning that this does not mean that the corresponding carrier relaxation rate also diverges. Indeed, as shown in Ref. 26 by means of a Monte Carlo simulation, the carrier thermalization rate via the screened classical c-c collisions is finite despite the divergent collisional rate.

With increasing screening our results (not presented) show a gradual deterioration of the classical analysis in comparison with the phase-shift analysis. Nevertheless, Fig. 10 demonstrates that for weak enough screening the classical analysis works very well or at least much better than the Born approximation. This is not surprising, because just this behavior is characteristic of the zero-screening limit.

[1] D. W. Snoke, W. W. Rühle, Y.-C. Lu, and E. Bauser, Phys. Rev. Lett. **68**, 990 (1992).
[2] J. B. Stark, W. H. Knox, and D. S. Chemla, Phys. Rev. Lett. **68**, 3080 (1992).
[3] A. Yacoby, V. Sivan, C. P. Umbach, and J. M. Hong, Phys. Rev. Lett. **64**, 1938 (1991).
[4] Th. Schäpers, M. Krüger, J. Appenzeller, A. Förster, B. Lengeler, and H. Lüth, Appl. Phys. Lett. **66**, 3603 (1995).
[5] R. A. Höpfel, J. Shah, P. A. Wolf, and A. C. Gossard, Phys. Rev. Lett. **56**, 2736 (1986).
[6] *Semiconductor Nanostructures: Physics and Device Applications*, edited by J. Shah (Academic, New York, 1992).
[7] M. Fischetti, S. E. Laux, and E. Crabbé, J. Appl. Phys. **78**, 1058 (1995).
[8] M. Grupen and K. Hess, Appl. Phys. Lett. **65**, 2454 (1994).
[9] N. W. Ashcroft and N. D. Mermin, *Solid State Physics* (Holt, Rinehart and Winston, New York, 1967).
[10] W. G. Baber, Proc. R. Soc. London, Ser. A **158**, 383 (1937).
[11] L. Landau and I. Pomeranschuk, Phys. Z. Sowjetunion **10**, L49 (1937).
[12] J. Quinn and R. A. Ferrel, Phys. Rev. **112**, 812 (1958).
[13] A. V. Chaplik, Zh. Éksp. Teor. Fiz. **60**, 1845 (1971) [Sov. Phys. JETP **33**, 997 (1971)]; G. F. Giuliani and J. J. Quinn, Phys. Rev. B **26**, 4421 (1982).
[14] L. Zheng and S. Das Sarma, Phys. Rev. B **53**, 9964 (1996); T. Jungwirth and A. H. MacDonald, *ibid.* **53**, 7403 (1996).
[15] M. G. Kane, K. W. Sun, and S. A. Lyon, Phys. Rev. B **50**, 7428 (1994).
[16] J. H. Collet and T. Ahmand, J. Phys. Chem. Solids **47**, 2933 (1988).
[17] J. H. Collet, Phys. Rev. B **47**, 10 279 (1993).
[18] M. Moško, A. Mošková, and V. Cambel, Phys. Rev. B **51**, 16 860 (1995).
[19] M. Moško and A. Mošková, Phys. Rev. B **44**, 10 794 (1991).
[20] L. Rota, P. Lugli, T. Elsaesser, and J. Shah, Phys. Rev. B **47**, 4226 (1993).
[21] D. W. Bailey, C. J. Stanton, and K. Hess, Phys. Rev. B **42**, 3423 (1990).
[22] M. Artaki and K. Hess, Phys. Rev. B **37**, 2933 (1988).
[23] A. Mošková and M. Moško, Phys. Rev. B **49**, 7443 (1994).
[24] A. Reklaitis, Phys. Lett. **88A**, 367 (1982).
[25] M. Reizer and J. W. Wilkins, Phys. Rev. B **55**, R7363 (1997).
[26] M. Moško and A. Mošková, Acta Phys. Pol. A **90**, 1055 (1996). There is a misprint in Eq. (1) of this paper (the misprint is not involved in the presented numerical calculations). A correct equation should be the same as Eq. (A1) of the present paper.
[27] M. Moško and P. Vagner, Phys. Rev. B **59**, R10445 (1999).
[28] Yu. M. Sirenko, V. Mitin, and P. Vasilopoulos, Phys. Rev. B **50**, 4631 (1994).
[29] M. Moško and V. Cambel, Phys. Rev. B **50**, 8864 (1994).
[30] L. D.Landau and E. M. Lifshits, *Nonrelativistic Quantum Mechanics* (Nauka, Moscow, 1989) (in Russian).
[31] M. Moško, D. Munzar, and P. Vagner, Phys. Rev. B **55**, 15 416 (1997).
[32] F. Stern and W. E. Howard, Phys. Rev. **163**, 816 (1967).
[33] *Handbook of Mathematical Functions*, edited by M. Abramowitz and I. Stegun (Dover, New York, 1971).
[34] A. Messiah, *Quantum Mechanics* (Wiley, New York, 1966).
[35] S. Kamiyama, K. Ohnaka, M. Suzuki, and T. Uenoyama, Jpn. J. Appl. Phys. **34**, 821 (1995).

[36] J. Ziman, *Principles of the Theory of Solids* (Cambridge University Press, Cambridge, 1964).

[37] For the treatment of screening in 2D systems see, e.g., F. Stern, Phys. Rev. Lett. **18**, 546 (1967); T. Ando, A. B. Fowler, and F. Stern, Rev. Mod. Phys. **54**, 437 (1982); L. Wendler, R. Haupt, and V. G. Grigoryan, Physica B **167**, 101 (1990); L. Wendler, F. Bechstedt, and M. Fiedler, Phys. Status Solidi B **159**, 143 (1990).

[38] S. M. Goodnick and P. Lugli, Phys. Rev. B **38**, 10 135 (1989).

[39] K. Kálna and M. Moško, Phys. Rev. B **54**, 17 730 (1996).

[40] A. Tomita, J. Shah, J. E. Cunningham, S. M. Goodnick, P. Lugli, and S. L. Chuang, Phys. Rev. B **48**, 5708 (1993); **52**, 5445 (1995).

[41] J. R. Meyer and F. J. Bartoli, Phys. Rev. B **23**, 5413 (1981).

[42] W. H. Press, S. A. Teukolsky, W. T. Vettering, and B. P. Flannery, *Numerical Recipes in Fortran* (Cambridge University Press, Cambridge, 1992).

[43] For $r\to\infty$ $J_m=\sqrt{4/\pi g r}\cos[(g/2)r-(\pi/2)m-(\pi/4)]$ and $Y_m=\sqrt{4/\pi g r}\sin[(g/2)r-(\pi/2)m-(\pi/4)]$ (see Ref. 33).

[44] It is not obvious that phase-shift analysis can work for $V(r)=q_\gamma q_\delta/(4\pi K r)$. The problem is that δ_m diverges for zero screening, which does not allow us to directly apply Eqs. (22)–(25) and Eq. (32). A more sophisticated procedure is needed. As pointed out in Ref. 30, what does not diverge is the difference $\delta_m-\delta_0$. If we evaluate $\delta_m-\delta_0$ from Eq. (24) numerically at $r \gg m/g$, we obtain a stable (r-independent) $\delta_m-\delta_0$. Once $\delta_m-\delta_0$ is known, the scattering amplitude can be calculated as follows. Multiplying the right-hand side of Eq. (32) by an extra factor $e^{-i2\delta_0}$ and applying the relation $\Sigma_{m=-\infty}^{\infty}e^{im\phi}=2\pi\delta(\phi)$, we change Eq. (32) into the formula $f(\phi,g)=(4i/\pi g)^{1/2}\Sigma_{m=-\infty}^{\infty}e^{i[m\phi+2(\delta_m-\delta_0)]}$, which depends on $\delta_m-\delta_0$ rather than on δ_m. If we insert that formula into Eqs. (5) and (6), these can be evaluated numerically [the factor $e^{-i2\delta_0}$ has no effect on Eqs. (5) and (6)].

[45] L. Kadanoff and G. Baym, *Quantum Statistical Mechanics* (Benjamin, New York, 1962).

[46] S. Hughes and T. Kobayshi, Semicond. Sci. Technol. **12**, 733 (1996).

[47] H. Haug and C. Ell, Phys. Rev. B **46**, 2126 (1992).

[48] D. TranThoai and H. Haug, Z. Phys. B: Condens. Matter **91**, 199 (1993).

[49] M. Bonitz, D. Kremp, D. Scott, R. Binder, W. Kraeft, and H. Kohler, J. Phys.: Condens. Matter **8**, 6057 (1996).

[50] R. Binder, H. Kohler, M. Bonitz, and N. Kwong, Phys. Rev. B **55**, 5110 (1997).

[51] W. Schafer, J. Opt. Soc. Am. B **13**, 1291 (1996).

[52] R. Binder and S. Koch, Prog. Quantum Electron. **19**, 307 (1995).

[53] D. Menashe and B. Laikhtman, Phys. Rev. B **54**, 11 561 (1996).

[54] E. Abrahams, Phys. Rev. **95**, 839 (1954).

[55] R. Balescu, *Equilibrium and Nonequilibrium Statistical Mechanics* (Wiley, New York, 1975).